E-Companion for Wang, Delage, and Coelho's "Data-driven Stochastic Vehicle Routing Problems with Deadlines under Decision-Dependent Travel Time"

EC.1. Algorithm Details

EC.1.1. Implementation of the LBBD Algorithm

Algorithm 1 describes the detailed procedure of the LBBD algorithm.

Algorithm 1: Logic-based Benders Decomposition Algorithm

Input A tolerance $\epsilon > 0$.

Initialize $\nu = 0$, $UB = +\infty$, $LB = -\infty$, $\mathcal{N} = \{o\}$, o has no branching constraints.

while *($\mathcal{N}$ is nonempty and $UB - LB > \epsilon$)* **do**

    $\nu = \nu + 1$.

    Select a node $o \in \mathcal{N}$, $\mathcal{N} \leftarrow \mathcal{N}/\{o\}$.

    Solve the LP relaxation of (MP) at the node o, obtain optimal solution $(\bar{\boldsymbol{x}}^{\nu}, \bar{\boldsymbol{s}}^{\nu})$ and optimal objective $lobj^{\nu}$.

    if $lobj^{\nu} < UB$ **then**

        if $(\bar{\boldsymbol{x}}^{\nu}, \bar{\boldsymbol{s}}^{\nu})$ *is integer* **then**

            For $\ell \in \mathcal{N}_d$, compute the expected delay obj^{ℓ} for $\bar{\boldsymbol{s}}^{\nu\ell}$.

            Add optimality cuts (8) to (MP).

            if $\sum_{\ell \in \mathcal{N}_d} obj^{\ell} \leq UB$ **then**

                $UB = \sum_{\ell \in \mathcal{N}_d} obj^{\ell}$, and $(\boldsymbol{x}^*, \boldsymbol{s}^*) = (\bar{\boldsymbol{x}}^{\nu}, \bar{\boldsymbol{s}}^{\nu})$.

            end

        end

        if $(\bar{\boldsymbol{x}}^{\nu}, \bar{\boldsymbol{s}}^{\nu})$ *is fractional* **then**

            Update $LB := \max\{LB, lobj^{\nu}\}$.

            Branch, resulting in nodes o^* and o^{**}, $\mathcal{N} \leftarrow \mathcal{N} \cup \{o^*, o^{**}\}$.

        end

    end

end

return UB and its corresponding optimal solution $(\boldsymbol{x}^*, \boldsymbol{s}^*)$.

EC.1.2. Warm Start

Algorithm 2 gives the outline of the warm starting procedure.

EC.1.3. Local Search

The local search procedures are provided in Algorithm 3.

EC.1.4. Determining the Value of ρ

Algorithm 4 gives an overview of the bisection method to determine the value of ρ.

Algorithm 2: Warm Start

Use the hybrid genetic search method to solve problem (10), and obtain feasible subpopulation $\{\boldsymbol{x}^m, \boldsymbol{s}^m\}_{m=1,\dots,M'}$.
Compute the expected delay obj^m of $(\boldsymbol{x}^m, \boldsymbol{s}^m)$ for $m = 1, \dots, M'$.
Let $m^* = \arg\min_{m=1,\dots,M'} obj^m$, and $\hat{\eta} = obj^{m^*}$.
Reorder the vehicle indices for $(\boldsymbol{x}^{m^*}, \boldsymbol{s}^{m^*})$ to satisfy the symmetry-breaking constraints.
return $(\boldsymbol{x}^{m^*}, \boldsymbol{s}^{m^*}, \hat{\eta})$.

Algorithm 3: Local Search Procedures

Input $(\bar{\boldsymbol{x}}, \bar{\boldsymbol{s}})$ and expected delay $\bar{obj}$.
Output $(\bar{\boldsymbol{x}}'', \bar{\boldsymbol{s}}'')$ and expected delay $\bar{obj}''$.
Find a solution $\bar{\boldsymbol{s}}'$ by improving $\bar{\boldsymbol{s}}$ with local search.
Let $\bar{obj}'$ be the expected delay based on $\bar{\boldsymbol{s}}'$.
if $\bar{obj}' < \bar{obj}$ **then**
    Construct $\bar{\boldsymbol{x}}'$ based on $\bar{\boldsymbol{s}}'$.
    Reorder the vehicle indices of $(\bar{\boldsymbol{x}}', \bar{\boldsymbol{s}}')$ to satisfy the symmetry-breaking constraints.
    Set $(\boldsymbol{x}'', \boldsymbol{s}'', obj'') := (\bar{\boldsymbol{x}}', \bar{\boldsymbol{s}}', \bar{obj}')$.
else
    Set $(\boldsymbol{x}'', \boldsymbol{s}'', obj'') := (\bar{\boldsymbol{x}}, \bar{\boldsymbol{s}}, \bar{obj})$.
end

Algorithm 4: Determining the value of ρ

Input A tolerance $\epsilon' > 0$, a small positive number ϵ''.
Initialize Upper bound $\bar{\rho}$ and lower bound $\underline{\rho}$.
$\rho = (\bar{\rho} + \underline{\rho})/2$.
Compute the probability:

$$\frac{\sum_{j=1}^{J'} \mathbf{1}\left\{\rho(1/(T+1))\sum_{t=1}^{T}(\sum_{a\in\mathcal{A}} \theta_a^t \hat{s}_a'^j + \bar{\theta}^t - \tau)^+ \le \mathbb{E}_{\mathbb{P}_{(\hat{s}'^j)}}\left[\left(\tilde{\xi} - \tau\right)^+\right]\right\}}{J'},$$

while $\bar{\rho} - \underline{\rho} > \epsilon''$ **do**
    if *the probability is larger than* ϵ' **then**
        $\underline{\rho} = \rho$ and $\rho = (\bar{\rho} + \underline{\rho})/2$.
    end
    else
        $\bar{\rho} = \rho$ and $\rho = (\bar{\rho} + \underline{\rho})/2$.
    end
end

EC.1.5. LBBD Algorithm with the Acceleration Strategies and Heuristic

Algorithm 5 presents the procedure of our implementation of the LBBD algorithm with the acceleration strategies and the lower bound heuristic.

Algorithm 5: Logic-based Benders Decomposition Algorithm

Input A tolerance $\epsilon > 0$.
Initialize $\nu = 0$, $UB = +\infty$, $LB = -\infty$, $\mathcal{N} = \{o\}$, o has no branching constraints.
$(\boldsymbol{x}^{m^*}, \boldsymbol{s}^{m^*}, \hat{\eta}) \Leftarrow$ Warm Start.
UB=$\hat{\eta}$, and set $\boldsymbol{x}^{m^*}, \boldsymbol{s}^{m^*}$ to be an initial solution for (MP).
while *($\mathcal{N}$ is nonempty and $UB - LB > \epsilon$)* **do**
  $\nu = \nu + 1$.
  Select a node $o \in \mathcal{N}$, $\mathcal{N} \leftarrow \mathcal{N}/\{o\}$.
  Solve the LP relaxation of (MP) at the node o, and obtain the optimal solution $(\bar{\boldsymbol{x}}^{\nu}, \bar{\boldsymbol{s}}^{\nu})$ and the optimal objective $lobj^{\nu}$.
  if $lobj^{\nu} < UB$ **then**
    if $(\bar{\boldsymbol{x}}^{\nu}, \bar{\boldsymbol{s}}^{\nu})$ *is an integer* **then**
      For $\ell \in \mathcal{N}_d$, we compute the expected delay $obj^{\nu\ell}$ for $\bar{\boldsymbol{s}}^{\nu\ell}$.
      $(\boldsymbol{x}'', \boldsymbol{s}'', obj'') \Leftarrow$ Local Search Procedure.
      Add the general optimality cut based on the solution $\boldsymbol{s}''$ to (MP).
      if $\sum_{\ell \in \mathcal{N}_d} obj''^{\ell} \leq UB$ **then**
        $UB = \sum_{\ell \in \mathcal{N}_d} obj''^{\ell}$, and $(\boldsymbol{x}^*, \boldsymbol{s}^*) = (\bar{\boldsymbol{x}}'', \bar{\boldsymbol{s}}'')$.
      end
    end
    if $(\bar{\boldsymbol{x}}^{\nu}, \bar{\boldsymbol{s}}^{\nu})$ *is fractional* **then**
      Update $LB := \max\{LB, lobj^{\nu}\}$.
      Branch, resulting in nodes o^* and o^{**}, $\mathcal{N} \leftarrow \mathcal{N} \cup \{o^*, o^{**}\}$.
    end
  end
end
return UB and its corresponding optimal solution $(\boldsymbol{x}^*, \boldsymbol{s}^*)$.

EC.2. Proof of Propositions and Lemmas

EC.2.1. Proof of Proposition 1

Let $\bar{\boldsymbol{s}}^{\nu}$ be a routing solution generated in the νth iteration for one of the vehicles. On a later iteration, if one vehicle's route does not start by visiting the first customer location of $\bar{\boldsymbol{s}}^{\nu}$, then the right-hand side of the cut (9) will be disabled. If it does start with the same location, then either the route ends there and thus the cut returns the right expected delay, or it pursues to a second destination. In the latter case, the second destination could be different from the route in $\bar{\boldsymbol{s}}^{\nu}$ thus disabling the cut, or pass by the same second stop. If the route is complete, then the cut returns the expected delays of a route that only goes to these two destinations. Otherwise, the equation pursues either canceling the cut or adding the right difference to recuperate the expected delay obtained if this was the last destination. Hence, the general optimality cuts (9) contain both the traditional optimality cut (8) together with all the optimality cuts for subroutes of $\bar{\boldsymbol{s}}^{\nu}$. They are therefore valid. $\square$

EC.2.2. Proof of Lemma 1

Given a $\boldsymbol{s}^\ell$ and $\ell \in \mathcal{N}_d$, from Shaked and Shanthikumar (2007), we have that first-order stochastic dominance implies

$$\mathbb{E}_{\mathbb{P}_{(\boldsymbol{s}^\ell)}}\left[\phi\left(\xi\right)\right] \geq \mathbb{E}_{\bar{\mathbb{P}}_{(\boldsymbol{s}^\ell)}}\left[\phi\left(\xi\right)\right], \text{ for all non-decreasing functions } \phi.$$

Let $\phi\left(\xi\right) = \left(\xi - \tau\right)^+$, which is non-decreasing, then

$$\mathbb{E}_{\mathbb{P}_{(\boldsymbol{s}^\ell)}}\left[\left(\xi - \tau\right)^+\right] \geq \mathbb{E}_{\bar{\mathbb{P}}_{(\boldsymbol{s}^\ell)}}\left[\left(\xi - \tau\right)^+\right].$$

Hence, (11c) is a relaxation of (11b). Therefore, problem (3) is equivalent to problem (11). □

EC.2.3. Proof of Lemma 2

Under the null hypothesis, one can first establish that since $\hat{F}_{Y|X}(y;x)$ is continuous we have that Z is uniformly distributed among $\{1,\ldots,K+1\}$. Namely, for all $k>1$:

$$\mathbb{P}(Z=k) = \mathbb{P}(\hat{Y}_{(k-1)}(X) < Y < \hat{Y}_{(k)}(X)) = 1/(K+1),$$

where $\hat{Y}_{(k)}(X)$ is the k-th smallest realization in the set $\{\hat{Y}(X)\}$, because all $\hat{Y}_k(X)$ and Y are i.i.d. given X. It therefore follows straightforwardly (see Pearson (1900)) that χ^2_K is a Pearson's cumulative test statistic for the multinomial distribution of $\sum_{i=1}^N \mathbf{1}\{z_i = k\}$. □

EC.3. Hypothesis Test on Endogenous Pairs of Arcs Travel Time

In this appendix, we investigate whether the endogeneity of arc travel time identified in Section 5.2 is due to the way that nodes are traversed, i.e., what pair of consecutive arcs are used on the route. This would indeed be the case if a customer were located near an intersection where right turns are faster than left turns. To do so, we apply a second set of Hoeffding's D independence tests to verify whether the time spent on pairs of consecutive arcs is independent of the length of the route. Specifically, for each historical route $i \in \{1,\cdots,N\}$ with the set of arcs: $\{(0,n^i_{(1)}),\cdots,(n^i_{(v_i)},j)\}$, where $n^i_{(k)} \in \mathcal{N}_c$ for $k \in \{1,\cdots,v_i\}$, and $j \in \mathcal{N}_d$, we consider pairs of the arcs, leading to $\{(0,n^i_{(1)},n^i_{(2)}),(n^i_{(1)},n^i_{(2)},n^i_{(3)}),\cdots,(n^i_{(v_i-1)},n^i_{(v_i)},j)\}$. Then the number of pairs for route i is v_i. For each arc pair $\bar{a}$ among all historical arc pairs, we gather the dataset $\{t^{\bar{a}}_i, v_i)\}_{i\in\mathcal{N}(\bar{a})}$, where $t^{\bar{a}}_i$ is the travel time of arc pair $\bar{a}$ in the route i, v_i is the size of route i, and $\mathcal{N}(\bar{a})$ is the set of routes containing the arc pair $\bar{a}$. The Hoeffding's D independence test compares the following hypotheses

- **Null hypothesis**: "The travel time on a pair of consecutive arcs is independent of the route length."
- **Alternative hypothesis**: "The travel time on a pair of consecutive arcs is dependent of the route length."

We set the significance threshold of the test to 5% and calculate p-values based on the non-parametric bootstrapping method described in Section 5.2. Focusing on the arc pairs that have more than 10 visits (i.e., $|\mathcal{N}(\bar{a})| \geq 10$), we observed a rejection rate of 26% (5 out of 19 arc pairs). The endogeneity of arc travel time appears therefore to still be present when accounting for the way that nodes are traversed. This finding supports the choice of a more sophisticated total travel time model than one that would simply predict total travel time based on a set of predictors for each pair of potential consecutive arcs.

EC.4. Additional Results for the Lower Bound Heuristic

We present additional experiments with the lower bound heuristic proposed in Section 4.3 to explore the tradeoff between the tightness of bounds and the risk of cutting off optimal solutions. Specifically, we use the experiment setting described in Section 5.5.1, and let the threshold $\varepsilon' \in \{0.55, 0.75, 0.85\}$, which is used to reduce the likelihood of introducing the incorrect lower bound cuts. Table EC.1 presents the average upper bound and estimated lower bound, the average absolute gap, the solution time for the instances that can be solved to optimality, the average time spent for the subproblem and local search procedures, the average number of cuts and nodes, and the optimal ratio for BDWLG_LH with different thresholds and service deadlines.

From Table EC.1 we observe that as the threshold ε' decreases, the likelihood of introducing incorrect cuts (12) increases, and consequently, the average estimated lower bound increases and the average absolute gap decreases significantly. The average optimal ratio is improved by about 42% when ε' varies from 0.85 to 0.55. In the meantime, the average upper bound increases modestly, leading to a slightly worse integer solution. Therefore, if we reduce the threshold ε' values, we can obtain better lower bound values and optimal ratios at the cost of slightly larger upper bound values. In reality, one could choose a proper threshold value based on their requirement on the likelihood of introducing correct cuts (12) and balance the lower and upper bound values.

Table EC.1 The average upper bound (UB) and estimated lower bound (Est_LB), the average absolute gap (Gap), the average solution time (in seconds) for the instances solved optimally (AvT), and subproblem and local search procedures (AvT_SP), the average number of cuts (# of cuts) and nodes (# of nodes), and the optimal ratio (Ratio) are reported.

ε'	τ	UB	Est_LB	Gap	AvT	AvT_SP	# of cuts	# of nodes	Ratio
	25	49.94	45.66	4.28	152.9	70.7	131	40,536	0.46
	35	19.49	17.28	2.21	146.1	65.8	127	54,566	0.46
0.55	45	5.53	4.65	0.88	170.8	71.8	212	74,498	0.42
	55	1.05	0.72	0.32	130.7	68.5	305	45,821	0.32
	65	0.12	0.03	0.09	75.2	41.0	229	14,791	0.46
	25	49.15	39.16	9.99	137.2	107.5	218	64,405	0.25
	35	19.12	14.17	4.95	158.4	96.0	206	73,846	0.30
0.75	45	5.40	3.60	1.80	131.3	98.0	310	79,045	0.26
	55	1.02	0.52	0.49	147.2	83.4	375	49,335	0.26
	65	0.11	0.02	0.09	88.3	51.8	289	17,161	0.44
	25	48.67	35.58	13.09	129.8	147.7	318	70,664	0.17
	35	18.7	12.58	6.12	156.3	122.1	277	74,460	0.21
0.85	45	5.35	3.11	2.24	183.5	122.1	395	78,170	0.20
	55	1.00	0.44	0.57	152.1	97.7	430	48,045	0.22
	65	0.1	0.01	0.09	170.2	59.7	293	14,553	0.45

EC.5. Computational Results for KDE Method

We present the lower bound heuristic and the computational results for KDE method in this section.

EC.5.1. Computational Results on Lower Bound Heuristic for KDE Method

Table EC.2 presents the lower bound probability, and the average absolute gap (in minutes) when the lower bound value is larger than the expected delay for the KDE method based on a newly generated set of routes with different numbers of locations.

Table EC.2 The lower bound probability and the average absolute gap (in minutes) are reported.

τ	25	35	45	55	65
LBProb	0.85	0.85	0.85	0.85	0.85
Avg_AGap	0.45	0.25	0.11	0.04	0.01

EC.5.2. Computational Results under KDE Method:

We present our results on the acceleration strategies and lower bound improvement heuristic implemented in the LBBD algorithm 5 for the data-driven VRP with the KDE method. In this section, we set the service deadline to be 55 minutes, which corresponds to the practical scenario (Liu et al. 2021). We illustrate the performance of the six different variants presented in Section 5.5.3. Table EC.3 shows the average upper bound and the estimated lower bound, the average absolute gap, the solution time for the instances that can be solved to optimality, the average time spent for the subproblem and local search procedures, the average number of cuts and nodes, and the optimal ratio for the KDE method, where the optimal ratio is computed as the number of solved instances over the total 440 instances.

Table EC.3 The average upper bound (UB) and estimated lower bound (Est_LB), the average absolute gap (Gap), the average solution time (in seconds) for the instances solved optimally (AvT), and subproblem and local search procedures (AvT_SP), the average number of cuts (# of cuts) and nodes (# of nodes), and the optimal ratio (Ratio) are reported.

Model	Method	UB	Est_LB	Gap	AvT	AvT_SP	# of cuts	# of nodes	Ratio
KDE	BDWLG_LH	0.17	0.10	0.07	104.0	72.0	782	29,847	0.39
	BDWLG	0.11	0.00	0.11	117.4	253.4	3,285	8,883	0.12
	BDWL	0.12	0.00	0.12	96.3	323.1	4,512	8,687	0.11
	BDW	2.60	0.00	2.60	N/A	3.8	20,278	21,774	0.00
	BD	2.87	0.00	2.87	N/A	3.8	20,388	22,282	0.00
	Genetic	0.78	0.00	0.78	N/A	N/A	N/A	N/A	0.04

Similar to Table 2, we can observe from Table EC.3 that BDWLG_LH achieves the smallest average absolute gap and largest optimal ratio among all the six methods, while BDWLG has a better average upper bound. For KDE, the improvement in the average absolute gap and the optimal ratio is about 40% and 69%, respectively. In addition, BDWL yields a slightly poor performance when compared with BDWLG, and BDWL has a significantly better performance than BDW. Furthermore, BDW outperforms BD. For KDE, BD and BDW perform worse than the genetic heuristic. The results from Table EC.3 further confirm the efficiency of the acceleration strategies and the lower bound heuristic proposed in Section 4.

EC.6. The Formulations and Solution Schemes of ALiu_{opt} and ALiu_{kNN}

Without loss of generality, in this paper, we assume that the travel time of arcs includes the service time at nodes. Then the assignment model proposed by Liu et al. (2021) is reduced to the following problem:

$$\underset{\boldsymbol{y}}{\text{minimize}} \sum_{\ell \in \mathcal{N}_d} (q_\ell - \tau)^+ \tag{EC.1a}$$

$$\text{subject to} \sum_{\ell \in \mathcal{N}_d} y_{i\ell} = 1, \qquad \forall i \in \mathcal{N}_c, \tag{EC.1b}$$

$$\sum_{i \in \mathcal{N}_c} d_i y_{i\ell} \leq Q, \qquad \forall \ell \in \mathcal{N}_d, \tag{EC.1c}$$

$$q_\ell = q(\boldsymbol{y}_\ell), \qquad \forall \ell \in \mathcal{N}_d, \tag{EC.1d}$$

$$y_{i\ell} \in \{0,1\}, \qquad \forall i \in \mathcal{N}_c, \ell \in \mathcal{N}_d, \tag{EC.1e}$$

where binary decision $y_{i\ell}$ is equal to one if customer location i is assigned to vehicle ℓ, zero otherwise. $q(\boldsymbol{y}_\ell)$ denotes a function of the customer locations served by driver ℓ that predict the total travel time by driver ℓ.

Following Liu et al. (2021), we also use LASSO as the prediction model, and the tractable predictors proposed by Liu et al. (2021) for the travel time. After linearizing each class of tractable predictors (see Liu et al. (2021) for more details), we can solve linear problem (EC.1).

Given the optimal assignment decision $\hat{y}_{i\ell}$ for customer $i \in \mathcal{N}_c$ and vehicle $\ell \in \mathcal{N}_d$, we want to optimize the route for each vehicle ℓ. Let set $\mathcal{I}_\ell := \{i \in \mathcal{N}_c : \hat{y}_{i\ell} = 1\}$ for all $\ell \in \mathcal{N}_d$, i.e., the set of customer locations that are assigned to vehicle ℓ, and set $\mathcal{J}_\ell := \{1, \ldots, |\mathcal{I}_\ell|\}$ denotes the set of positions for vehicle ℓ. Binary decision $z^\ell_{ij} = 1$ if customer i is assigned to position j for vehicle ℓ.

In order to use the LBBD algorithm to solve the routing model for $\ell \in \mathcal{N}_d$, we first define the following master problem:

$$\underset{\boldsymbol{\eta}, \boldsymbol{z}}{\text{minimize}} \; \eta_\ell, \tag{EC.2a}$$

$$\text{subject to} \sum_{i \in \mathcal{I}_\ell} z^\ell_{ij} = 1, \qquad \forall j \in \mathcal{J}_\ell, \tag{EC.2b}$$

$$\sum_{j \in \mathcal{J}_\ell} z^\ell_{ij} = 1, \qquad \forall i \in \mathcal{I}_\ell, \tag{EC.2c}$$

$$z^\ell_{ij} \in \{0,1\}, \qquad \forall i \in \mathcal{I}_\ell, j \in \mathcal{J}_\ell. \tag{EC.2d}$$

$$\eta_\ell \geq 0. \tag{EC.2e}$$

The constraints guarantee that each customer is assigned to one position, and each position is allotted to only one customer, and customer i can be assigned to a position belonging to ℓ only if i is assigned to vehicle ℓ. Given $\hat{z}^\ell_{ij}$ from the master problem (EC.2), let

$$\bar{\mathcal{J}}^i_\ell = \{j \in \mathcal{J}_\ell \big| \hat{z}^\ell_{ij} = 1\}.$$

We can also extract the corresponding route $\hat{\boldsymbol{s}}^\ell$. For ALiu$_{\text{opt}}$, we use CGMM to generate $N' = 10,000$ samples $\bar{\xi}^i_\ell$ and let the expected delay for vehicle $\ell \in \mathcal{N}_d$ be $lobj_\ell = \frac{1}{N'}\sum_{i=1}^{N'}\left(\bar{\xi}^i_\ell - \tau\right)^+$. We then add the following optimality cut to the master problem:

$$\eta_\ell \geq lobj_\ell - lobj_\ell \sum_{i\in\mathcal{I}_\ell}\sum_{j\in\bar{\mathcal{J}}^i_\ell}(1 - z^\ell_{ij}) \tag{EC.3}$$

We can also use the kNN method to optimize the routing decision, i.e., ALiu$_{\text{kNN}}$. We use the kNN method to define the discrete probability $p_i(\hat{\boldsymbol{s}}^\ell)$, then $lobj_\ell = \sum_{i=1}^{N(\hat{\boldsymbol{s}}^\ell)} p_i(\hat{\boldsymbol{s}}^\ell)\left(\xi^i(\hat{\boldsymbol{s}}^\ell) - \tau\right)^+$.

EC.7. The Formulations and Solution Schemes of kNN$_{\text{SArc}}$ and kNN$_{\text{DArc}}$

Given the historical arc travel times $\{\hat{t}^1, \cdots, \hat{t}^{N_t}\}$, where $\hat{t}^i \in \mathbb{R}^+$ represents the historical arc travel time, and N_t is the number of historical arc travel times (in the training dataset $N_t = 9620$). We use the non-parametric methods with the features proposed in Section 3 to estimate the distribution of arc travel time $\mathbb{P}_{\tilde{t}_a}$ for each arc $a \in \mathcal{A}$, i.e.,

$$\mathbb{P}_{\tilde{t}_a} = \sum_{i=1}^{N_t(a)} p_i(a)\delta_{\hat{t}^i(a)},$$

where $N_t(a)$, $p_i(a)$ and $\hat{t}^i(a)$ are the number of scenarios, the probability and the arc travel time for scenario $i \in \{1, \cdots, N_t(a)\}$. We assume that the distributions for arc travel times are independent, then the stochastic arc-based VRP model with the arc travel time distributions can be reformulated as:

$$\underset{(\boldsymbol{x},\boldsymbol{s})\in\mathcal{S}}{\text{minimize}} \sum_{\ell\in\mathcal{N}_d} \mathbb{E}_{\mathbb{P}_{\tilde{t}}}\left(\left(\sum_{a\in\mathcal{A}} \tilde{t}_a s^\ell_a - \tau\right)^+\right) \tag{EC.4}$$

with $\mathbb{P}_{\tilde{t}} := \prod_{a\in\mathcal{A}} \mathbb{P}_{\tilde{t}_a}$ as the product measure.

The computational cost of solving the linear programming representation of problem (EC.4) is prohibitive since the number of scenarios to consider is exponential in $|\mathcal{A}|$. To efficiently solve the problem (EC.4), we propose to use the LBBD algorithm. Specifically, given a feasible solution $(\bar{\boldsymbol{x}}, \bar{\boldsymbol{s}})$ of the MP (6), we compute the expected delay $obj^\ell(\boldsymbol{s}^\ell) := \mathbb{E}_{\mathbb{P}_{\tilde{t}}}\left[\left(\sum_{a\in\mathcal{A}} \tilde{t}^i_a s^\ell_a - \tau\right)^+\right]$ and add the corresponding optimality cuts and general optimality cuts to the MP (6). However, the number of scenarios is still exponential in the length of the route, thus making the evaluation of $obj^\ell(\boldsymbol{s}^\ell)$ prohibitively computationally demanding. Instead of expanding the full scenario tree, we generate an approximation of the total travel

Algorithm 6: Computing the expected delay for route $\bar{\boldsymbol{s}}^\ell$

Input A tolerance $\varepsilon > 0$, a set of arcs $\{a_1, \cdots, a_{v_\ell}\}$ in route $\bar{\boldsymbol{s}}^\ell$ with the number of customer locations v_ℓ, a range $[\underline{t}, \bar{t}]$ for the support of all $\tilde{t}_a$.

Initialize Discretization $\mathcal{E} : \{\underline{t}v_\ell + k\varepsilon : k \in \{0, \ldots, \lceil v_\ell(\bar{t} - \underline{t})/\varepsilon \rceil\}\}$, and $q^0 \in \mathbb{R}_+^{|\mathcal{E}|}$ with $q^0(\xi) := \mathbf{1}\{\xi = v_\ell \underline{t}\}$.

for $k = 1 : v_\ell$ **do**

$\quad q^k(\xi) := \sum_{\xi' \in \mathcal{E}} \sum_{i=1}^{N_t(a_k)} q^{k-1}(\xi') p_i(a_k) \mathbf{1}\{\xi' + \hat{t}^i(a) - \underline{t} \in [\xi - \varepsilon/2, \xi + \varepsilon/2)\}$ for all $\xi \in \mathcal{E}$.

end

Return $obj^\ell \approx \sum_{\xi \in \mathcal{E}} q^{v_\ell}(\xi)(\xi - \tau)^+$.

time distribution using a fixed discretization of the range from the minimum to the maximum total possible travel time, using steps of fixed size $\varepsilon > 0$. Algorithm 6 describes the algorithm used to estimate the expected delay $obj^\ell(\boldsymbol{s}^\ell)$.

We could also solve the following deterministic arc-based VRP model (EC.5) based on the average arc travel time $\bar{t}_a = \sum_{i=1}^{N_t(a)} p_i(a)\hat{t}^i(a)$:

$$\underset{(\boldsymbol{x},\boldsymbol{s}) \in \mathcal{S}}{\text{minimize}} \sum_{\ell \in \mathcal{N}_d} \left(\sum_{a \in \mathcal{A}} \bar{t}_a s_a^\ell - \tau \right)^+, \tag{EC.5}$$

which is a standard VRP model.

For the out-of-sample performance, we first choose the non-parametric models for the arc travel time distribution estimation. Specifically, we also use the cross-validation method to select the best hyper-parameters for the kNN and KDE models with the training data. We found that the average cross-validation root MSE for the kNN and KDE methods are equal to 5.55 and 5.67, respectively. Compared with the KDE method, the kNN method also achieves lower error. Therefore, we also use the kNN method to estimate the distributions of the arc travel times.

EC.8. Generalization to Data-Driven DRO-VRP Formulation

We now extend the data-driven stochastic VRP model (3) to a DRO framework, where we use the Wasserstein metric to construct a ball in the space of probability distributions centered at the distribution $\mathbb{P}_{(\boldsymbol{s}^\ell)}$. A data-driven DRO-VRP model that minimizes the worst-case expected delay thus can take the form:

$$\underset{(\boldsymbol{x},\boldsymbol{s}) \in \mathcal{S}}{\text{minimize}} \sum_{\ell \in \mathcal{N}_d} \left[\sup_{\mathbb{Q} \in \mathbb{B}_\epsilon(\mathbb{P}_{(\boldsymbol{s}^\ell)})} \mathbb{E}_{\mathbb{Q}} \left(\tilde{\xi} - \tau \right)^+ \right], \tag{EC.6}$$

where

$$\mathbb{B}_\epsilon(\mathbb{P}_{(\boldsymbol{s}^\ell)}) := \left\{ \mathbb{Q} \in \mathcal{M}(\Xi) : d_W(\mathbb{P}_{(\boldsymbol{s}^\ell)}, \mathbb{Q}) \leq \epsilon \right\},$$

with $\mathcal{M}(\Xi)$ as the set of probability measures on the support $\Xi := \mathbb{R}_+$, and $d_W : \mathcal{M}(\Xi) \times \mathcal{M}(\Xi) \to \mathbb{R}_+$ is the Wasserstein metric defined as

$$d_W(\mathbb{Q}_1, \mathbb{Q}_2) := \left(\inf_{\Pi \in \Gamma(\mathbb{Q}_1,\mathbb{Q}_2)} \int_{\Xi^2} |\xi_1 - \xi_2|^q \Pi(\mathrm{d}\xi_1, \mathrm{d}\xi_2) \right)^{1/q}$$

for all distributions $\mathbb{Q}_1, \mathbb{Q}_2 \in \mathcal{M}(\Xi)$, $\Gamma(\mathbb{Q}_1, \mathbb{Q}_2)$ is a set of all joint probability with marginals $\mathbb{Q}_1$ and $\mathbb{Q}_2$. Radius $\epsilon \in \mathbb{R}^+$, Wasserstien order $q \in [1, \infty)$.

We first examine the following inner worst-case expectation problem in (EC.6):

$$\sup_{\mathbb{Q} \in \mathbb{B}_\epsilon(\mathbb{P}_{(\boldsymbol{s}^\ell)})} \mathbb{E}_{\mathbb{Q}} \left(\tilde{\xi} - \tau \right)^+. \tag{EC.7}$$

By leveraging Theorem 4.2 in Esfahani and Kuhn (2018), we obtain the strong dual of the worst-case expectation problem (EC.7) over the Wasserstein ambiguity set, which is centered at the endogenous distribution on the training samples in Lemma EC.1.

LEMMA EC.1. *For a given* $(\boldsymbol{x}, \boldsymbol{s}) \in \mathcal{S}$, *the strong dual of the worst-case expectation problem* (EC.7) *is*

$$\inf_{\lambda \geq 0} \lambda \epsilon^q + \sum_{i=1}^{N(\boldsymbol{s}^\ell)} p_i(\boldsymbol{s}^\ell) \sup_{\tilde{\xi} \in \Xi} \left[(\tilde{\xi} - \tau)^+ - \lambda |\tilde{\xi} - \xi_i(\boldsymbol{s}^\ell)|^q \right]. \tag{EC.8}$$

Proof. Our proof mainly leverages Theorem 4.2 of Esfahani and Kuhn (2018), which extends the uniform distribution on the training samples to the endogenous distribution. Based on Theorem 4.2 in Esfahani and Kuhn (2018), we have that

$$\begin{aligned}
\sup_{\mathbb{Q} \in \mathbb{B}_\epsilon(\mathbb{P}_{(\boldsymbol{s}^\ell)})} \mathbb{E}_{\mathbb{Q}} \left(\tilde{\xi} - \tau \right)^+ &= \begin{cases} \sup\limits_{\mathbb{Q}_i \in \mathcal{M}(\Xi)} & \displaystyle\sum_{i=1}^{N(\boldsymbol{s}^\ell)} p_i(\boldsymbol{s}^\ell) \int_\Xi (\xi - \tau)^+ \mathbb{Q}_i(d\xi) \\ \text{subject to} & \displaystyle\sum_{i=1}^{N(\boldsymbol{s}^\ell)} p_i(\boldsymbol{s}^\ell) \int_\Xi |\xi - \xi_i(\boldsymbol{s}^\ell)|^q \mathbb{Q}_i(d\xi) \leq \epsilon^q \end{cases} \\
&= \sup_{\mathbb{Q}_i \in \mathcal{M}(\Xi)} \inf_{\lambda \geq 0} \sum_{i=1}^{N(\boldsymbol{s}^\ell)} p_i(\boldsymbol{s}^\ell) \int_\Xi (\xi - \tau)^+ \mathbb{Q}_i(d\xi) \\
&\quad + \lambda \left(\epsilon^q - \sum_{i=1}^{N(\boldsymbol{s}^\ell)} p_i(\boldsymbol{s}^\ell) \int_\Xi |\xi - \xi_i(\boldsymbol{s}^\ell)|^q \mathbb{Q}_i(d\xi) \right) \\
&\leq \inf_{\lambda \geq 0} \sup_{\mathbb{Q}_i \in \mathcal{M}(\Xi)} \lambda \epsilon^q + \sum_{i=1}^{N(\boldsymbol{s}^\ell)} p_i(\boldsymbol{s}^\ell) \int_\Xi \left[(\xi - \tau)^+ - \lambda |\xi - \xi_i(\boldsymbol{s}^\ell)|^q \right] \mathbb{Q}_i(d\xi)
\end{aligned}$$

$$= \inf_{\lambda \geq 0} \lambda \epsilon^q + \sum_{i=1}^{N(\boldsymbol{s}^\ell)} p_i(\boldsymbol{s}^\ell) \sup_{\xi \in \Xi} \left[(\xi - \tau)^+ - \lambda |\xi - \xi_i(\boldsymbol{s}^\ell)|^q \right].$$

The inequality is in fact an equality for any $\epsilon \geq 0$ (Esfahani and Kuhn 2018). $\square$

In the following, we consider the two possible cases, $q = 1$ and $q > 1$, separately.

EC.8.1. Case: $q = 1$

We first introduce the following definition of the growth rate to guarantee that the inner supremum of the dual reformulation is finite.

Definition EC.1. (Growth rate, Gao and Kleywegt (2016)). The growth rate κ is defined as

$$\kappa := \inf \left\{ \lambda \geq 0 : \sum_{i=1}^{N(\boldsymbol{s}^\ell)} p_i(\boldsymbol{s}^\ell) \sup_{\xi \in \Xi} \left[(\xi - \tau)^+ - \lambda |\xi - \xi_i(\boldsymbol{s}^\ell)| \right] < \infty \right\}$$

Under Definition EC.1, we can obtain the exact value of the inner supremum problem in Lemma EC.2.

Lemma EC.2. *For a given $(\boldsymbol{x}, \boldsymbol{s}) \in \mathcal{S}$, we have the growth rate $\kappa = 1$. Let $f_i(\xi) := (\xi - \tau)^+ - \lambda |\xi - \xi_i(\boldsymbol{s}^\ell)|$, if $\lambda \geq \kappa$, then $\sup_{\xi \in \Xi} f_i(\xi)$ is attained at $\xi_i(\boldsymbol{s}^\ell)$.*

Proof. There are two cases: $\xi_i(\boldsymbol{s}^\ell) \geq \tau$ or $\xi_i(\boldsymbol{s}^\ell) < \tau$.

When $\xi_i(\boldsymbol{s}^\ell) \geq \tau$:

- if $\xi \geq \xi_i(\boldsymbol{s}^\ell) \geq \tau$, then $f_i(\xi) = (\xi - \tau) - \lambda(\xi - \xi_i(\boldsymbol{s}^\ell))$, which implies that

$$\sup_{\xi \geq \xi_i(\boldsymbol{s}^\ell)} f_i(\xi) = \begin{cases} f_i(\xi_i(\boldsymbol{s}^\ell)), & \text{if } \lambda \geq 1, \\ +\infty, & \text{otherwise.} \end{cases}$$

- if $\xi_i(\boldsymbol{s}^\ell) \geq \xi \geq \tau$, then $f_i(\xi) = (\xi - \tau) - \lambda(\xi_i(\boldsymbol{s}^\ell) - \xi)$, and $\sup_{\xi \in [\tau, \xi_i(\boldsymbol{s}^\ell)]} f_i(\xi) = f_i(\xi_i(\boldsymbol{s}^\ell))$.
- if $\xi_i(\boldsymbol{s}^\ell) \geq \tau \geq \xi$, then $f_i(\xi) = -\lambda(\xi_i(\boldsymbol{s}^\ell) - \xi)$, and $\sup_{\xi \leq \tau} f_i(\xi) = -\lambda(\xi_i(\boldsymbol{s}^\ell) - \tau) \leq f_i(\xi_i(\boldsymbol{s}^\ell))$.

Therefore, when $\xi_i(\boldsymbol{s}^\ell) \geq \tau$, $\sup_{\xi \in \Xi} f_i(\xi) = f_i(\xi_i(\boldsymbol{s}^\ell)) < \infty$ if $\lambda \geq 1$ and infinite if $\lambda < 1$.

The case when $\xi_i(\boldsymbol{s}^\ell) < \tau$ is similar. Namely,

- if $\xi \geq \tau$, then $f_i(\xi) = (\xi - \tau) - \lambda(\xi - \xi_i(\boldsymbol{s}^\ell))$, which implies that

$$\sup_{\xi \geq \tau} f_i(\xi) = \begin{cases} f_i(\tau), & \text{if } \lambda \geq 1, \\ +\infty, & \text{otherwise.} \end{cases}$$

- if $\tau \geq \xi \geq \xi_i(\boldsymbol{s}^\ell)$, then $f_i(\xi) = -\lambda(\xi - \xi_i(\boldsymbol{s}^\ell))$, and $\sup_{\xi \in [\xi_i(\boldsymbol{s}^\ell), \tau]} f_i(\xi) = f_i(\xi_i(\boldsymbol{s}^\ell)) \geq f_i(\tau)$.

- if $\xi_i(\boldsymbol{s}^\ell) \geq \xi$, then $f_i(\xi) = -\lambda(\xi_i(\boldsymbol{s}^\ell) - \xi)$, and $\sup_{\xi \leq \xi_i(\boldsymbol{s}^\ell)} f_i(\xi) = f_i(\xi_i(\boldsymbol{s}^\ell))$.

Thus, $\sup_{\xi \in \Xi} f_i(\xi) = f_i(\xi_i(\boldsymbol{s}^\ell))$ when $\lambda \geq 1$ and otherwise equal to ∞. This confirms that the growth rate is $\kappa = 1$. $\square$

THEOREM EC.1. *When $q = 1$, the optimal objective value of the dual reformulation is:*

$$\sum_{i=1}^{N(\boldsymbol{s}^\ell)} p_i(\boldsymbol{s}^\ell)(\xi_i(\boldsymbol{s}^\ell) - \tau)^+ + \epsilon.$$

Hence, the data-driven DRO-VRP model is equivalent to the stochastic VRP model (3)*.*

Proof. From Lemma EC.2, we obtain the following closed-form expression of problem (EC.8).

$$\begin{aligned} &\inf_{\lambda \geq 0} \lambda\epsilon + \sum_{i=1}^{N(\boldsymbol{s}^\ell)} p_i(\boldsymbol{s}^\ell) \sup_{\xi \in \Xi} \left[(\xi - \tau)^+ - \lambda|\xi - \xi_i(\boldsymbol{s}^\ell)|\right] \\ =& \inf_{\lambda \geq 1} \lambda\epsilon + \sum_{i=1}^{N(\boldsymbol{s}^\ell)} p_i(\boldsymbol{s}^\ell)(\xi_i(\boldsymbol{s}^\ell) - \tau)^+ = \epsilon + \sum_{i=1}^{N(\boldsymbol{s}^\ell)} p_i(\boldsymbol{s}^\ell)(\xi_i(\boldsymbol{s}^\ell) - \tau)^+. \end{aligned}$$

Thus, the data-driven DRO-VRP model with the Wasserstein order $q = 1$ is equivalent to the stochastic VRP model (3) in terms of set of optimal solutions, whereas the optimal values are offset by ϵ. $\square$

EC.8.2. Case: $q > 1$

In the $q > 1$ case, we also obtain a closed-form expression for the inner worst-case expectation problem (EC.7). We first analyze the inner supremum problem in Lemma EC.3.

LEMMA EC.3. *For a given $(\boldsymbol{x}, \boldsymbol{s}) \in \mathcal{S}$, let $f_i(\xi) := (\xi - \tau)^+ - \lambda|\xi - \xi_i(\boldsymbol{s}^\ell)|^q$. If $\lambda > 0$, then*

$$\sup_{\xi \in \Xi} f_i(\xi) = \begin{cases} 0, & \text{if } i \in N_1, \\ \xi_i(\boldsymbol{s}^\ell) - \tau + \dfrac{q-1}{q}(\dfrac{1}{\lambda q})^{\frac{1}{q-1}}, & \text{if } i \in N_2. \end{cases}$$

where $N_1 = \left\{i \in N(\boldsymbol{s}^\ell) : \tau - \frac{q-1}{q}(\frac{1}{\lambda q})^{\frac{1}{q-1}} > \xi_i(\boldsymbol{s}^\ell)\right\}$ *and* $N_2 = \left\{i \in N(\boldsymbol{s}^\ell) : \tau - \frac{q-1}{q}(\frac{1}{\lambda q})^{\frac{1}{q-1}} \leq \xi_i(\boldsymbol{s}^\ell)\right\}$.

Proof. When $\xi_i(\boldsymbol{s}^\ell) \leq \tau$,

- If $\xi \leq \tau$, $\sup_{\xi \leq \tau} f_i(\xi) = \sup_{\xi \leq \tau} -\lambda|\xi - \xi_i(\boldsymbol{s}^\ell)|^q = 0$ occurs at $\xi = \xi_i(\boldsymbol{s}^\ell)$.

- If $\xi > \tau$, then $f_i(\xi) = \xi - \tau - \lambda\left(\xi - \xi_i(\boldsymbol{s}^\ell)\right)^q$, and the derivative $f_i'(\xi)$ is:

$$f_i'(\xi) = 1 - \lambda q\left(\xi - \xi_i(\boldsymbol{s}^\ell)\right)^{q-1}.$$

By letting $f_i'(\xi) = 0$, we can have $\xi = (\frac{1}{\lambda q})^{\frac{1}{q-1}} + \xi_i(\boldsymbol{s}^\ell)$. If $(\frac{1}{\lambda q})^{\frac{1}{q-1}} + \xi_i(\boldsymbol{s}^\ell) > \tau$, then $\sup_{\xi\geq\tau} f_i(\xi) = f_i((\frac{1}{\lambda q})^{\frac{1}{q-1}} + \xi_i(\boldsymbol{s}^\ell)) = \xi_i(\boldsymbol{s}^\ell) + (\frac{1}{\lambda q})^{\frac{1}{q-1}} - \tau - \lambda(\frac{1}{\lambda q})^{\frac{q}{q-1}} = \xi_i(\boldsymbol{s}^\ell) - \tau + \frac{q-1}{q}(\frac{1}{\lambda q})^{\frac{1}{q-1}}$. The latter is non-negative if and only if $i \in N_2$. If $(\frac{1}{\lambda q})^{\frac{1}{q-1}} + \xi_i(\boldsymbol{s}^\ell) \leq \tau$, then $\sup_{\xi\geq\tau} f_i(\xi) = -\lambda|\tau - \xi_i(\boldsymbol{s}^\ell)|^q \leq 0$.

This implies that:

$$\sup_{\xi\in\Xi} f_i(\xi) = \begin{cases} 0, & \text{if } i \in N_1, \\ \xi_i(\boldsymbol{s}^\ell) - \tau + \dfrac{q-1}{q}(\dfrac{1}{\lambda q})^{\frac{1}{q-1}}, & \text{if } i \in N_2. \end{cases}$$

When $\xi_i(\boldsymbol{s}^\ell) > \tau$,

- if $\xi \geq \xi_i(\boldsymbol{s}^\ell)$, then $f_i(\xi) = \xi - \tau - \lambda\left(\xi - \xi_i(\boldsymbol{s}^\ell)\right)^q$. Hence, $\sup_{\xi\geq\xi_i(\boldsymbol{s}^\ell)} f_i(\xi) = \xi_i(\boldsymbol{s}^\ell) - \tau + \frac{q-1}{q}(\frac{1}{\lambda q})^{\frac{1}{q-1}} \geq \xi_i(\boldsymbol{s}^\ell) - \tau \geq 0$
- if $\tau \leq \xi \leq \xi_i(\boldsymbol{s}^\ell)$, then $f_i(\xi) = \xi - \tau - \lambda\left(\xi_i(\boldsymbol{s}^\ell) - \xi\right)^q$, and the derivative $f_i'(\xi)$ is:

$$f_i'(\xi) = 1 + \lambda q\left(\xi_i(\boldsymbol{s}^\ell) - \xi\right)^{q-1}.$$

Since $f_i'(\xi) > 0$, $\sup_{\xi\in[\tau,\xi_i(\boldsymbol{s}^\ell)]} f_i(\xi) = f_i(\xi_i(\boldsymbol{s}^\ell)) = \xi_i(\boldsymbol{s}^\ell) - \tau$.

- if $\xi < \tau$, then $f_i(\xi) = -\lambda\left(\xi_i(\boldsymbol{s}^\ell) - \xi\right)^q$. Therefore, $\sup_{\xi\leq\tau} f_i(\xi) = f_i(\tau) = 0 \leq \xi_i(\boldsymbol{s}^\ell) - \tau$

We therefore have that $\sup_{\xi\in\Xi} f_i(\xi) = \xi_i(\boldsymbol{s}^\ell) - \tau + \frac{q-1}{q}(\frac{1}{\lambda q})^{\frac{1}{q-1}} \geq 0$. Since $\xi_i(\boldsymbol{s}^\ell) > \tau$ implies that $i \in N_2$, the condition is well covered by the definition in the lemma. □

From Lemma EC.3, the objective function of dual formulation (EC.8) can be rewritten as follows:

$$\begin{aligned} g(\lambda) :=& \lambda\epsilon^q + \sum_{i=1}^{N(\boldsymbol{s}^\ell)} p_i(\boldsymbol{s}^\ell) \sup_{\xi\in\Xi}\left[(\xi-\tau)^+ - \lambda|\xi - \xi_i(\boldsymbol{s}^\ell)|^q\right] \\ =& \lambda\epsilon^q + \sum_{i\in N_2} p_i(\boldsymbol{s}^\ell)\left[\xi_i(\boldsymbol{s}^\ell) - \tau + (\frac{1}{\lambda q})^{\frac{1}{q-1}}(\frac{q-1}{q})\right]. \end{aligned}$$

Without loss of generality, we assume that the historical data $\{\xi_1(\boldsymbol{s}^\ell), \cdots, \xi_{N(\boldsymbol{s}^\ell)}(\boldsymbol{s}^\ell)\}$ is sorted in nondecreasing order. We let $\xi_0(\boldsymbol{s}^\ell) = 0$, $\xi_{N(\boldsymbol{s}^\ell)+1}(\boldsymbol{s}^\ell) = +\infty$, $i^* = \max\{i \in \{0, \cdots, N(\boldsymbol{s}^\ell)\} : \xi_i(\boldsymbol{s}^\ell) < \tau\}$. The following theorem shows the optimal objective value for the dual reformulation (EC.8).

THEOREM EC.2. *The optimal objective value of the dual reformulation* (EC.8) *is*

$$\inf_{\lambda>0} g(\lambda) = \begin{cases} \min\left\{\min\limits_{k\in\{0,\cdots,i^*\}} H_1(k), H_2(i^*+1)\right\}, & \text{if } h(i^*+1) > \xi_{i^*}(\boldsymbol{s}^\ell),\\ \min\left\{\min\limits_{k\in\{0,\cdots,i^*\}} H_1(k), H_2(1)\right\}, & \text{if } h(1) < \xi_0(\boldsymbol{s}^\ell),\\ \min\left\{\min\limits_{k\in\{0,\cdots,i^*\}} H_1(k), H_2(k^*)\right\}, & \text{if } \exists k^* \in \{1,\cdots,i^*\}, h(k^*) \in (\xi_{k^*-1}(\boldsymbol{s}^\ell), \xi_{k^*}(\boldsymbol{s}^\ell)],\\ \min\left\{\min\limits_{k\in\{0,\cdots,i^*\}} H_1(k)\right\}, & \text{otherwise,} \end{cases}$$

where $h(k) = \tau - \epsilon(\sum_{i=k}^{N(\boldsymbol{s}^\ell)} p_i(\boldsymbol{s}^\ell))^{-\frac{1}{q}}(\frac{q-1}{q})$, $H_1(k) := (\frac{\Delta}{\tau-\xi_k(\boldsymbol{s}^\ell)})^{q-1}\epsilon^q + \sum_{i=k+1}^{N(\boldsymbol{s}^\ell)} p_i(\boldsymbol{s}^\ell)\left[\xi_i(\boldsymbol{s}^\ell) - \xi_k(\boldsymbol{s}^\ell)\right]$, $H_2(k) := \epsilon(\sum_{i=k}^{N(\boldsymbol{s}^\ell)} p_i(\boldsymbol{s}))^{\frac{q-1}{q}} + \sum_{i=k}^{N(\boldsymbol{s}^\ell)} p_i(\boldsymbol{s}^\ell)\left[\xi_i(\boldsymbol{s}^\ell) - \tau\right]$, $\Delta = (\frac{1}{q})^{\frac{1}{q-1}}(\frac{q-1}{q})$, *and* $\sum_{i=N(\boldsymbol{s}^\ell)+1}^{N(\boldsymbol{s}^\ell)} = 0$.

Proof. For $k \in \{1,\cdots,i^*\}$, when $(\frac{\Delta}{\tau-\xi_{k-1}(\boldsymbol{s}^\ell)})^{q-1} < \lambda \le (\frac{\Delta}{\tau-\xi_k(\boldsymbol{s}^\ell)})^{q-1}$, that is $\xi_{k-1}(\boldsymbol{s}^\ell) < \tau - (\frac{1}{\lambda})^{\frac{1}{q-1}}\Delta \le \xi_k(\boldsymbol{s}^\ell)$, we have

$$g(\lambda) = \lambda\epsilon^q + \sum_{i\in\{k,\cdots,N(\boldsymbol{s}^\ell)\}} p_i(\boldsymbol{s}^\ell)\left[\xi_i(\boldsymbol{s}^\ell) - \tau + (\frac{1}{\lambda q})^{\frac{1}{q-1}}(\frac{q-1}{q})\right].$$

The subgradient of $g'(\lambda)$ is $\epsilon^q - \sum_{i\in\{k,\cdots,N(\boldsymbol{s}^\ell)\}} p_i(\boldsymbol{s}^\ell)(\frac{1}{q})^{\frac{q}{q-1}}\lambda^{-\frac{q}{q-1}}$. By letting $g'(\lambda) = 0$, we obtain $\lambda = (\epsilon)^{1-q}q^{-1}(\sum_{i\in\{k,\cdots,N(\boldsymbol{s}^\ell)\}} p_i(\boldsymbol{s}^\ell))^{\frac{q-1}{q}}$. Thus,

$$\inf g(\lambda) = \begin{cases} (\frac{\Delta}{\tau-\xi_k(\boldsymbol{s}^\ell)})^{q-1}\epsilon^q + \sum\limits_{i=k+1}^{N(\boldsymbol{s}^\ell)} p_i(\boldsymbol{s}^\ell)\left[\xi_i(\boldsymbol{s}^\ell) - \xi_k(\boldsymbol{s}^\ell)\right], & \text{if } \tau - \epsilon(\sum\limits_{i=k}^{N(\boldsymbol{s}^\ell)} p_i(\boldsymbol{s}^\ell))^{-\frac{1}{q}}(\frac{q-1}{q}) > \xi_k(\boldsymbol{s}^\ell),\\ (\frac{\Delta}{\tau-\xi_{k-1}(\boldsymbol{s}^\ell)})^{q-1}\epsilon^q + \sum\limits_{i=k}^{N(\boldsymbol{s}^\ell)} p_i(\boldsymbol{s}^\ell)\left[\xi_i(\boldsymbol{s}^\ell) - \xi_{k-1}(\boldsymbol{s}^\ell)\right], & \text{if } \tau - \epsilon(\sum\limits_{i=k}^{N(\boldsymbol{s}^\ell)} p_i(\boldsymbol{s}^\ell))^{-\frac{1}{q}}(\frac{q-1}{q}) \le \xi_{k-1}(\boldsymbol{s}^\ell),\\ \epsilon(\sum\limits_{i=k}^{N(\boldsymbol{s}^\ell)} p_i(\boldsymbol{s}))^{\frac{q-1}{q}} + \sum\limits_{i=k}^{N(\boldsymbol{s}^\ell)} p_i(\boldsymbol{s}^\ell)(\xi_i(\boldsymbol{s}^\ell) - \tau), & \text{otherwise.} \end{cases}$$

Let $h(k) = \tau - \epsilon(\sum_{i=k}^{N(\boldsymbol{s}^\ell)} p_i(\boldsymbol{s}^\ell))^{-\frac{1}{q}}(\frac{q-1}{q})$.

If there exists a $k^* \in \{1,\cdots,i^*\}$ satisfies $h(k^*) \in (\xi_{k^*-1}(\boldsymbol{s}^\ell), \xi_{k^*}(\boldsymbol{s}^\ell)]$, when $k > k^*$, $h(k) \le h(k^*) \le \xi_{k^*}(\boldsymbol{s}^\ell) \le \xi_{k-1}(\boldsymbol{s}^\ell)$. Therefore, for $k \in \{k^*+1,\cdots,i^*\}$, when $(\frac{\Delta}{\tau-\xi_{k-1}(\boldsymbol{s}^\ell)})^{q-1} < \lambda \le (\frac{\Delta}{\tau-\xi_k(\boldsymbol{s}^\ell)})^{q-1}$, we have

$$\inf g(\lambda) = (\frac{\Delta}{\tau-\xi_{k-1}(\boldsymbol{s}^\ell)})^{q-1}\epsilon^q + \sum_{i=k}^{N(\boldsymbol{s}^\ell)} p_i(\boldsymbol{s}^\ell)\left[\xi_i(\boldsymbol{s}^\ell) - \xi_{k-1}(\boldsymbol{s}^\ell)\right].$$

Similarly, for $k \in \{1, \cdots, k^* - 1\}$, when $(\frac{\Delta}{\tau - \xi_{k-1}(\boldsymbol{s}^\ell)})^{q-1} < \lambda \le (\frac{\Delta}{\tau - \xi_k(\boldsymbol{s}^\ell)})^{q-1}$, we have

$$\inf g(\lambda) = (\frac{\Delta}{\tau - \xi_k(\boldsymbol{s}^\ell)})^{q-1} \epsilon^q + \sum_{i=k+1}^{N(\boldsymbol{s}^\ell)} p_i(\boldsymbol{s}^\ell) \left[\xi_i(\boldsymbol{s}^\ell) - \xi_k(\boldsymbol{s}^\ell)\right],$$

and k^* is unique if it exists. When $\lambda > (\frac{\Delta}{\tau - \xi_{i^*}(\boldsymbol{s}^\ell)})^{q-1}$, $N_2 = \{i^* + 1, \cdots, N(\boldsymbol{s}^\ell)\}$, and

$$g(\lambda) = \lambda \epsilon^q + \sum_{i=i^*+1}^{N(\boldsymbol{s}^\ell)} p_i(\boldsymbol{s}^\ell) \left[\xi_i(\boldsymbol{s}^\ell) - \tau + (\frac{1}{\lambda q})^{\frac{1}{q-1}} (\frac{q-1}{q})\right].$$

By letting $g'(\lambda) = 0$, we have $\lambda = (\epsilon)^{1-q} q^{-1} (\sum_{i=i^*+1}^{N(\boldsymbol{s}^\ell)} p_i(\boldsymbol{s}^\ell))^{\frac{q-1}{q}}$ if $i^* < N(\boldsymbol{s}^\ell)$, and

$$\inf g(\lambda) = \begin{cases} \epsilon(\sum_{i=i^*+1}^{N(\boldsymbol{s}^\ell)} p_i(\boldsymbol{s}))^{\frac{q-1}{q}} + \sum_{i=i^*+1}^{N(\boldsymbol{s}^\ell)} p_i(\boldsymbol{s}^\ell)(\xi_i(\boldsymbol{s}^\ell) - \tau), & \text{if } \tau - \epsilon(\sum_{i=i^*+1}^{N(\boldsymbol{s}^\ell)} p_i(\boldsymbol{s}^\ell))^{-\frac{1}{q}} (\frac{q-1}{q}) > \xi_{i^*}(\boldsymbol{s}^\ell), \\ (\frac{\Delta}{\tau - \xi_{i^*}(\boldsymbol{s}^\ell)})^{q-1} \epsilon^q + \sum_{i=i^*+1}^{N(\boldsymbol{s}^\ell)} p_i(\boldsymbol{s}^\ell) \left[\xi_i(\boldsymbol{s}^\ell) - \xi_{i^*}(\boldsymbol{s}^\ell)\right], & \text{otherwise.} \end{cases}$$

Since $h(i^* + 1) \le \xi_{i^*}(\boldsymbol{s}^\ell)$, when $\lambda > (\frac{\Delta}{\tau - \xi_{i^*}(\boldsymbol{s}^\ell)})^{q-1}$, we have

$$\inf g(\lambda) = (\frac{\Delta}{\tau - \xi_{i^*}(\boldsymbol{s}^\ell)})^{q-1} \epsilon^q + \sum_{i=i^*+1}^{N(\boldsymbol{s}^\ell)} p_i(\boldsymbol{s}^\ell) \left[\xi_i(\boldsymbol{s}^\ell) - \xi_{i^*}(\boldsymbol{s}^\ell)\right].$$

If $i^* = N(\boldsymbol{s}^\ell)$, we also have

$$\inf g(\lambda) = (\frac{\Delta}{\tau - \xi_{i^*}(\boldsymbol{s}^\ell)})^{q-1} \epsilon^q + \sum_{i=i^*+1}^{N(\boldsymbol{s}^\ell)} p_i(\boldsymbol{s}^\ell) \left[\xi_i(\boldsymbol{s}^\ell) - \xi_{i^*}(\boldsymbol{s}^\ell)\right].$$

Similarly, when $\lambda \le (\frac{\Delta}{\tau - \xi_0(\boldsymbol{s}^\ell)})^{q-1}$, we have

$$\inf g(\lambda) = (\frac{\Delta}{\tau - \xi_0(\boldsymbol{s}^\ell)})^{q-1} \epsilon^q + \sum_{i=1}^{N(\boldsymbol{s}^\ell)} p_i(\boldsymbol{s}^\ell) \left[\xi_i(\boldsymbol{s}^\ell) - \xi_0(\boldsymbol{s}^\ell)\right].$$

Overall, if k^* exists, we have $\inf_{\lambda > 0} g(\lambda) = \min\{\min_{k \in \{0, \cdots, i^*\}} H_1(k), H_2(k^*)\}$.

If $h(i^* + 1) > \xi_{i^*}(\boldsymbol{s}^\ell)$, then k^* does not exist, $\inf g(\lambda) = \min\{\min_{k \in \{0, \cdots, i^*\}} H_1(k)\}$ for $\lambda \le (\frac{\Delta}{\tau - \xi_{i^*}(\boldsymbol{s}^\ell)})^{q-1}$, and $\inf g(\lambda) = \min\{\min_{k \in \{0, \cdots, i^*\}} H_1(k), H_2(i^* + 1)\}$. In this situation, if $i^* = N$, $h(i^* + 1) = -\infty$ and $h(i^* + 1) < \xi_{i^*}(\boldsymbol{s}^\ell)$.

If $h(i^* + 1) \le \xi_{i^*}(\boldsymbol{s}^\ell)$ and k^* does not exist, then $\inf g(\lambda) = \min\{\min_{k \in \{0, \cdots, i^*\}} H_1(k)\}$ for $\lambda > (\frac{\Delta}{\tau - \xi_0(\boldsymbol{s}^\ell)})^{q-1}$, and if $h(1) < \xi_0$, we have $\inf g(\lambda) = \min\{\min_{k \in \{0, \cdots, i^*\}} H_1(k), H_2(1)\}$, else $\inf g(\lambda) = \min\{\min_{k \in \{0, \cdots, i^*\}} H_1(k)\}$. $\square$

EC.8.3. Solution Scheme for the DRO-VRP model

For the solution scheme, the LBBD algorithm proposed in Section 4 can also be used to solve the DRO-VRP model (EC.6). Specifically, given a feasible solution $(\bar{\boldsymbol{x}}, \bar{\boldsymbol{s}})$ of (MP), let the expected delay obj^ℓ equal to the optimal objective value of problem (EC.7), it is easy to verify that the optimality cuts, general optimality cuts, warm starting and local search procedures proposed in Section 4 are also valid for the DRO-VRP model (EC.6). In terms of the lower bound heuristic, from Lemma EC.4 we have that the master problem (15) can also be used to solve the DRO-VRP model (EC.6).

LEMMA EC.4. *For all $(\boldsymbol{x}, \boldsymbol{s}) \in \mathcal{S}$, let the distribution of $\tilde{\xi}$ under some $\bar{\mathbb{P}}_{(\cdot)}$ be uniformly first-order stochastically dominated by its distribution under $\mathbb{P}_{(\cdot)}$, i.e.*

$$\bar{\mathbb{P}}_{(\boldsymbol{s}^\ell)}(\tilde{\xi} \le z) \ge \mathbb{P}_{(\boldsymbol{s}^\ell)}(\tilde{\xi} \le z)\,, \forall z \in \mathbb{R}, \forall \ell \in \mathcal{N}_d, \forall (\boldsymbol{x}, \boldsymbol{s}) \in \mathcal{S},$$

then problem (EC.6) *is equivalent to the following problem:*

$$\underset{(\boldsymbol{x},\boldsymbol{s})\in\mathcal{S},\boldsymbol{\eta}}{\text{minimize}} \sum_{\ell\in\mathcal{N}_d} \eta_\ell \tag{EC.9a}$$

$$\text{subject to } \eta_\ell \ge \sup_{\mathbb{Q}\in\mathbb{B}_\epsilon(\mathbb{P}_{(\boldsymbol{s}^\ell)})} \mathbb{E}_{\mathbb{Q}}\left[\left(\tilde{\xi} - \tau\right)^+\right], \qquad \forall \ell \in \mathcal{N}_d, \tag{EC.9b}$$

$$\eta_\ell \ge \mathbb{E}_{\bar{\mathbb{P}}_{(\boldsymbol{s}^\ell)}}\left[\left(\tilde{\xi} - \tau\right)^+\right], \qquad \forall \ell \in \mathcal{N}_d. \tag{EC.9c}$$

Proof. Given a $\boldsymbol{s}^\ell$ and $\ell \in \mathcal{N}_d$, from constraint (EC.9b), we have that

$$\eta_\ell \ge \mathbb{E}_{\mathbb{P}_{(\boldsymbol{s}^\ell)}}\left[\left(\tilde{\xi} - \tau\right)^+\right], \ \ \forall \ell \in \mathcal{N}_d.$$

By applying Lemma 1, the following constraints hold:

$$\mathbb{E}_{\mathbb{P}_{(\boldsymbol{s}^\ell)}}\left[(\xi - \tau)^+\right] \ge \mathbb{E}_{\bar{\mathbb{P}}_{(\boldsymbol{s}^\ell)}}\left[(\xi - \tau)^+\right].$$

Hence, (EC.9c) is a relaxation of (EC.9b). Therefore, problem (EC.6) is equivalent to problem (EC.9). $\square$

We conclude that the LBBD algorithm with the enhancements is also applicable for solving the DRO-VRP model (EC.6). Given that this paper focuses on providing an efficient algorithm for the data-driven stochastic VRP formulation (3), we leave the question of how to accelerate the algorithm for the DRO-VRP model (EC.6) open for further research.

EC.8.4. Out-of-Sample Performance

The experiment setting is also analogous to the setting used in Section 5.5.1 with the service deadline $\tau \in \{45, 55, 65\}$. We let $q = 2$, and the radius ϵ is selected using a k-fold cross-validation scheme. Specifically, we randomly split the training dataset into three equal-sized groups. One of the groups is used as the validation set for calculating the out-of-sample expected delays, and the remaining groups are used as the training set. The cross-validation process is repeated three times, and at each time, we solve the DRO-VRP model with batches that contain less than 20 customer locations. At the end of the process, the ϵ value with the minimum average expected delay over three times is used. Figure EC.1 presents the statistics of the out-of-sample expected delay for the data-driven stochastic VRP model with the kNN method (kNN) and the DRO-VRP model with the kNN method (kNN_{DRO}).

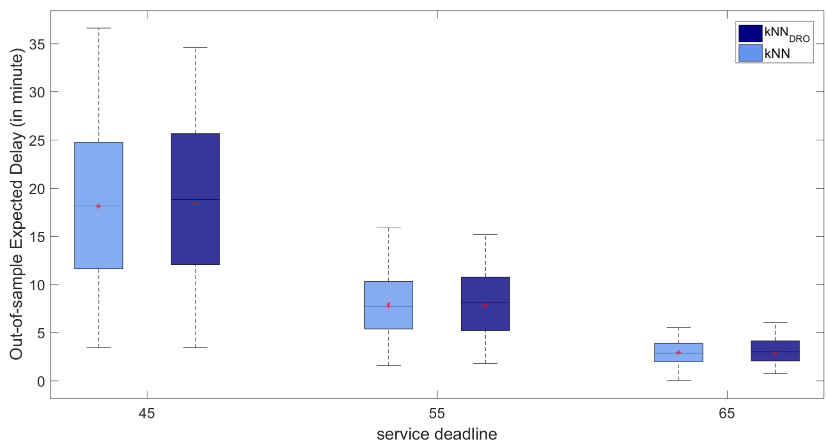

Figure EC.1 **Statistics of the out-of-sample expected delay for the data-driven VRP with kNN method (kNN), and the DRO-VRP model with the kNN method. The red star identifies the mean of the out-of-sample expected delay.**

From Figure EC.1 we observe that compared to the stochastic data-driven VRP, the DRO-VRP model reduces the maximum value of out-of-sample expected delay by about 5.5% when $\tau = 45$, and 4.7% when $\tau = 55$. While for the other statistics of the out-of-sample expected delay, the DRO-VRP model has a comparable performance to the stochastic data-driven VRP.

EC.9. Illustrative Example of Effect of Route Area on Expected Delays

Figure EC.2 presents a spatial representation of the assignment decisions for a batch instance with high out-of-sample total expected delay when the service deadline $\tau = 55$. We observed from this figure that the assignment decisions obtained from our kNN method are usually concentrated on the sides of the service region. Conversely, several assignments from $\mathrm{kNN}_{\mathrm{SArc}}$ and $\mathrm{kNN}_{\mathrm{DArc}}$ methods exhibit a high degree of spatial dispersion. As a result, kNN achieves an average value of S that is about 84% lower than the average S produced by the routes of $\mathrm{kNN}_{\mathrm{DArc}}$ and $\mathrm{kNN}_{\mathrm{SArc}}$. We also observe for this batch that the kNN method improves the out-of-sample expected delay by about 52%.

References

Esfahani PM, Kuhn D (2018) Data-driven distributionally robust optimization using the wasserstein metric: Performance guarantees and tractable reformulations 171:115–166.

Liu S, He L, Max Shen ZJ (2021) On-time last-mile delivery: Order assignment with travel-time predictors. *Management Science* 67(7):4095–4119.

Pearson K (1900) X. on the criterion that a given system of deviations from the probable in the case of a correlated system of variables is such that it can be reasonably supposed to have arisen from random sampling. *The London, Edinburgh, and Dublin Philosophical Magazine and Journal of Science* 50(302):157–175.

Shaked M, Shanthikumar JG (2007) Stochastic Orders. *New York, NY: Springer New York*.

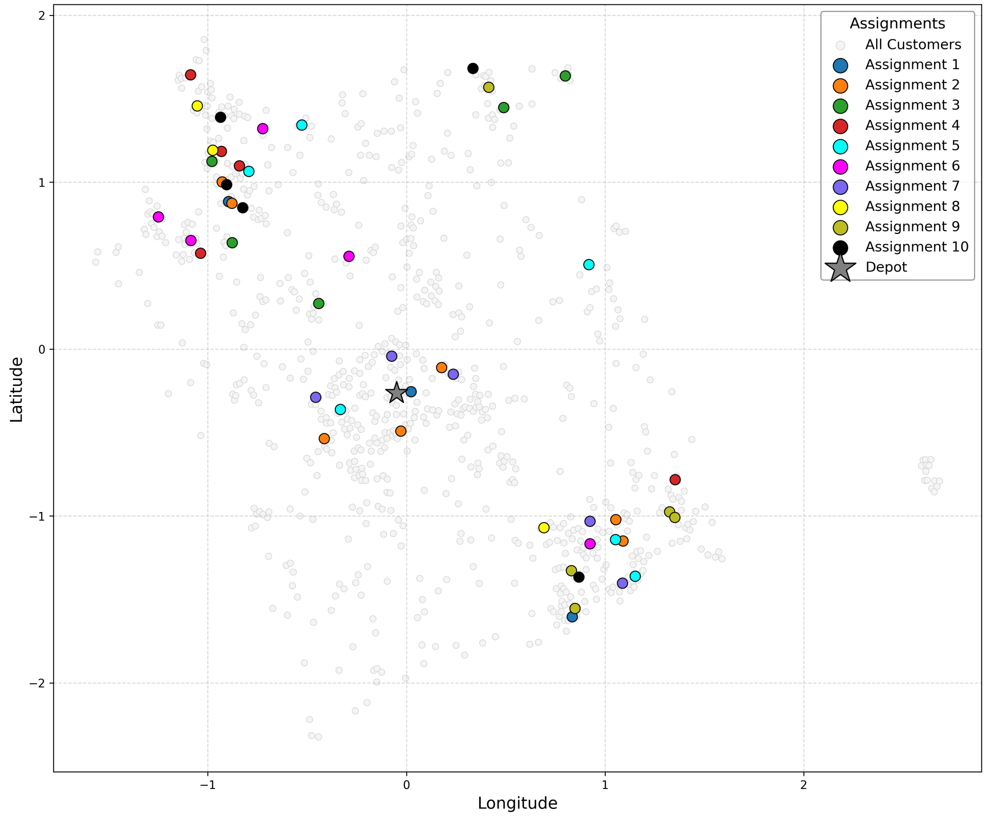
Assignments
All Customers
Assignment 1
Assignment 2
Assignment 3
Assignment 4
Assignment 5
Assignment 6
Assignment 7
Assignment 8
Assignment 9
Assignment 10
Depot
Latitude
Longitude
2
1
0
−1
−2
−1
0
1
2

(a)

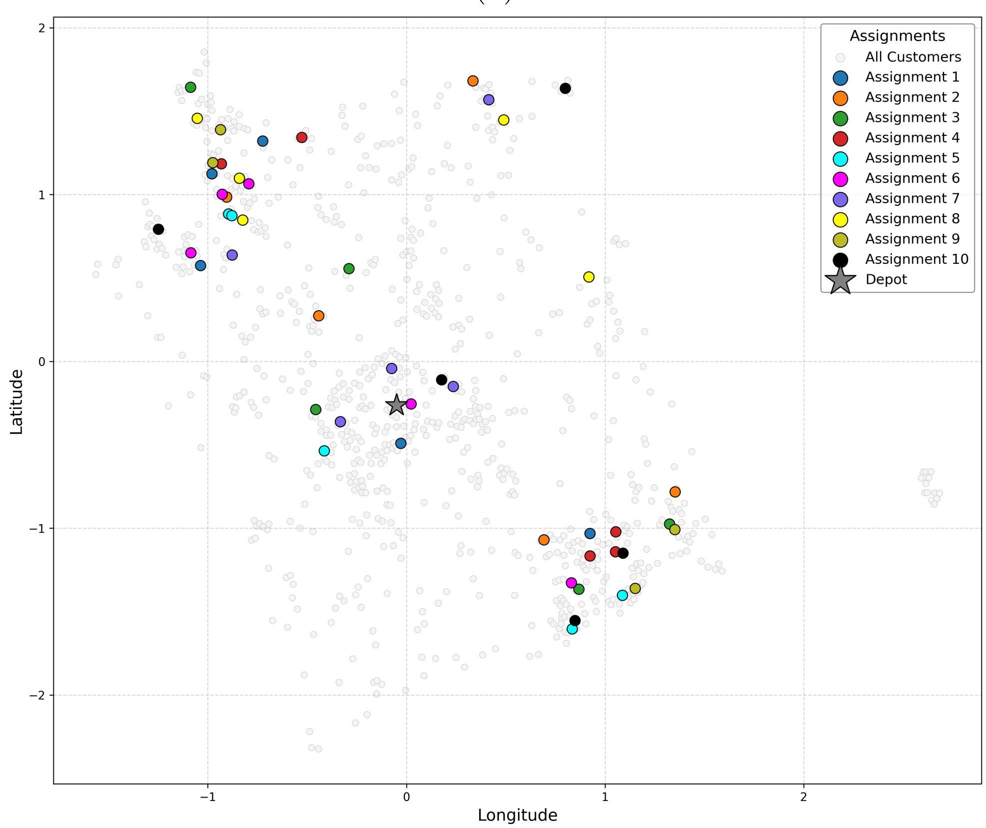
Assignments
All Customers
Assignment 1
Assignment 2
Assignment 3
Assignment 4
Assignment 5
Assignment 6
Assignment 7
Assignment 8
Assignment 9
Assignment 10
Depot
Latitude
Longitude
2
1
0
−1
−2
−1
0
1
2

(b)

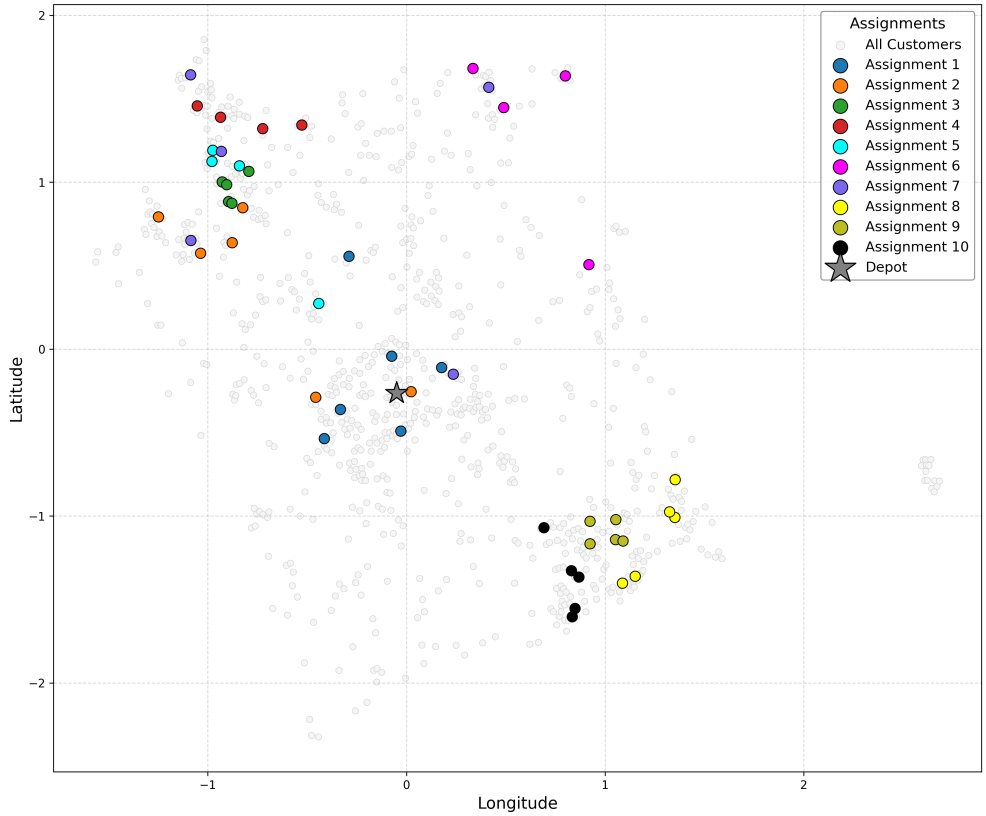

(c)

Figure EC.2 Comparison of assignment decisions in an illustrative example: (a) kNN$_{\text{DArc}}$ with average route area of 4.2 and expected delay of 23, (b) kNN$_{\text{SArc}}$ with average route area of 5.0 and expected delay of 34, and (c) presents kNN with average route area of 0.7 and expected delay of 13.